

OFDR multi-core fiber strain vector sensing for underwater environment

Junhua Zhang
Electronic Information Engineering
Wuhan University of Technology and
Shanghai Jiao Tong University
Wuhan, China
299118@whut.edu.cn

Mingxing Lv
State Key Laboratory of Advanced
Optical Communication Systems and
Networks
Shanghai Jiao Tong University
Shanghai, China
1120034910186@sjtu.edu.cn

Xinwan Li
State Key Laboratory of Advanced
Optical Communication Systems and
Networks
Shanghai Jiao Tong University
Shanghai, China
lixinwan@sjtu.edu.cn

Abstract—In this paper, multi-core fiber combined with IQ modulated optical frequency domain reflectometer (OFDR) system scheme is proposed for strain vector sensing in water and the maximum error after correction for the measured curvature is 1.71%.

Keywords—underwater strain vector sensing, multi-core fiber, Optical frequency domain reflectometer system, distributed optical fiber sensing

I. INTRODUCTION

The ocean environment is extremely complex and faces a series of technical challenges such as difficulties in high-capacity communication, wide-area exploration and long-time operation. Underwater submersibles have become an important means and tool for conducting deep-sea exploration. However, due to the complex and ever-changing deep-sea environment, ensuring the safety of submersibles has become a major challenge in deep-sea exploration. Once the submersible loses its own position information and gets lost in the deep sea, it will bring unpredictable losses.

For cable-connected Remote Operated Vehicle (ROV), there is a natural convergence advantage between optical fibers and umbilical cables, which can be directly utilized by connecting submersibles with the umbilical cable, combined with wired technology, to meet the positioning needs of current deep-sea submersibles. Therefore, underwater positioning based on multi-core fiber has important research value and application potential.

This paper proposes a structure for distributed strain vector sensing based on multi-core fiber, combined with an IQ-modulated OFDR system scheme[1], which realizes the perception of strain vector and has been preliminarily validated underwater.

II. PRINCIPLE OF STRAIN VECTOR SENSING

When the multi-core fiber is strained and bent, because of the symmetry of the spatial structure of the core arrangement, when the core is strained at the same place, the magnitude of the strain on each core is not uniform[2], that is, some cores are stretched, some cores are compressed, and the direction of force on each core is different. According to the magnitude of the strain on each core and the different direction of the strain, the strain vector information of the multi-core fiber at the point can be obtained through mathematical calculation, including strain curvature and strain direction.

As shown in Fig. 1, each core of the seven-core fiber is numbered, the middle core is numbered 1, and the rest of the outer core is numbered counterclockwise. And core No. 1 to core No. 7 direction as the x-axis positive direction, perpendicular to the x-axis, pointing to core No. 2 and Core No. 3 direction as the Y-axis positive direction. θ_i is the angle between the first core of the outer layer and the center of the seven-core fiber relative to the positive direction of the x-axis. When the fiber is subjected to the direction of the strain vector, the corresponding direction of the strain vector is θ_b .

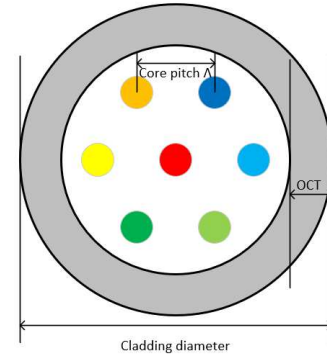


Fig. 1. Diagram of multi-core fiber axes

When the multi-core fiber is bent, the bending strain at any point on the fiber core i can be described as[3]:

$$\varepsilon_i = -\frac{r_i}{R} \cos(\theta_b - \theta_i) \quad (1)$$

where ε_i is the local strain in core i , R is the bending radius, r_i is the distance between core i and the center of the fiber. To calculate curvature ($\kappa = 1/R$) using information from all cores and reduce the sensitivity to error in a single strain measurement, we define an apparent curvature vector which points in the direction of the i^{th} core from the center of the fiber[3], [4]:

$$\kappa_{app,i} = -\frac{\varepsilon_i}{r_i} (\cos \theta_i \mathbf{j} + \sin \theta_i \mathbf{k}) \quad (2)$$

where unit vectors \mathbf{j} and \mathbf{k} align with the local x- and y-axes, respectively. For N number of cores in the fiber, the vector sum of the apparent curvature vectors is formulated as:

$$\kappa_{app} = -\sum_{i=1}^N \frac{\varepsilon_i}{r_i} \cos \theta_i j - \sum_{i=1}^N \frac{\varepsilon_i}{r_i} \sin \theta_i k \quad (3)$$

For the symmetric case in which each core is distance r from the center of the fiber, substituting (2) for the strain and applying trigonometric identities gives[5], [6]:

$$\kappa = \frac{2|\kappa_{app}|}{N} = \frac{2\sqrt{\left(\sum_{i=1}^N \varepsilon_i \cos \theta_i\right)^2 + \left(\sum_{i=1}^N \varepsilon_i \sin \theta_i\right)^2}}{Nr} \quad (4)$$

The corresponding direction of the strain vector is then:

$$\theta_b = \text{angle}(\kappa_{app}) \quad (5)$$

At this point, the magnitude of the bending strain is measured experimentally, and through (5), the direction angle of the strain at this point can be calculated, and finally the perception of the strain vector can be realized.

III. EXPERIMENT SETUP

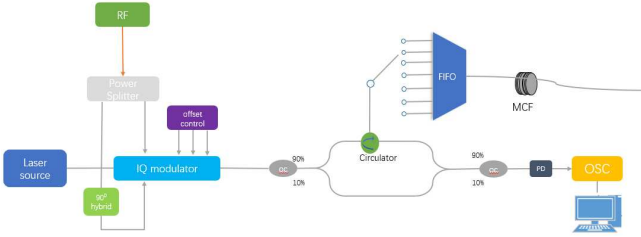


Fig. 2. OFDR distributed fiber strain vector sensing system diagram based on IQ modulation

The experimental setup depicted in Fig. 2, the laser emits narrow linewidth single-frequency laser, and the linear sweep light is modulated by IQ modulating module, the light is divided into two paths in the 90:10 coupler OC1. 10% of the light enters the reference fiber as the reference light, 90% of the light enters the seven-core fiber through the loop, and the seven-core fiber separates the different cores through the Fan-In Fan-Out (FIFO) module, single-mode fiber tails are respectively connected and numbered 1 ~ 7 core. After entering from the loop, the sweep light is respectively selected to be connected to the core 1 ~ 7 for measurement, the backscattered Rayleigh light of different cores is coherently beat in OC2 by loop and reference light, then received by Photoelectric detector (PD) and collected by oscilloscope. The multi-core fiber is tested under water to verify the detection ability and error range of the fiber bending strain at different depth. Due to the difference between underwater environment and free space, different pressure levels exist at different depth underwater, so the pressure on the optical fiber from water varies at different depth. As a result, placing a bent optical fiber underwater will result in differences in its sensing capability and system performance compared to free space. The underwater state of the multi-core fiber is shown in Fig. 3. Wrap it around a circular ring with a radius of 9.5cm and fix it after winding it 8 times. Then, place it underwater and connect the other end of the optical fiber to the OFDR system shown in Fig. 2 for experimental measurements.

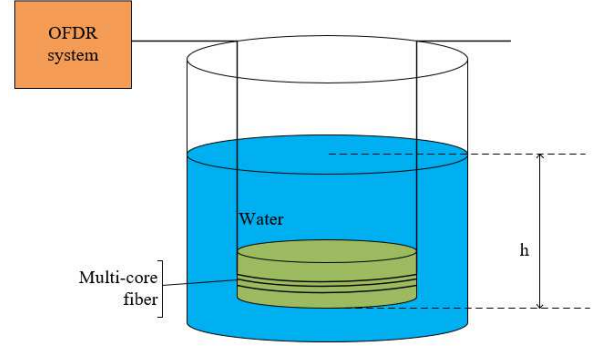


Fig. 3. Diagram of multi-core fiber in water environment

Using FIFO to select one of the optical fibers in the multi-core fiber, perform experimental measurements as shown in Fig. 3. The edge of the water bucket is marked with a scale of 0 to 25cm, and subsequent measurements will be taken at intervals of 5cm to study the signal and data at different water depth.

IV. EXPERIMENTAL RESULTS

As described above, the multi-core fiber was placed at depths of 0cm, 5cm, 10cm, 15cm, 20cm, and 25cm for experimental verification and comparison. Specifically, the bending strain vector information of the multi-core fiber was first measured in free space, i.e. at the 0cm. Then, the optical fibers were placed at a depth of 5cm in water, and the Rayleigh scattering signals of each fiber core were measured. The cross-correlation operation was performed with the Rayleigh scattering signals of the optical fiber in free space to obtain the frequency shift at each position of the seven-core optical fiber[7], [8]. According to the magnitude of the frequency shift and the principle of multi-core fiber strain vector sensing, the curvature magnitude and bending direction at each position can be obtained[9]. Keeping the fiber winding method and number of turns constant, the above experimental operation was repeated at depths of 10cm, 15cm, 20cm, and 25cm underwater to obtain the curvature values at different depth, as shown in Fig. 4. The horizontal axis represents the position of the scattering point on the fiber ring, and the vertical axis represents the curvature value. The mean curvature values of the optical fiber at different depths in water were then calculated and the results are shown in Table I.

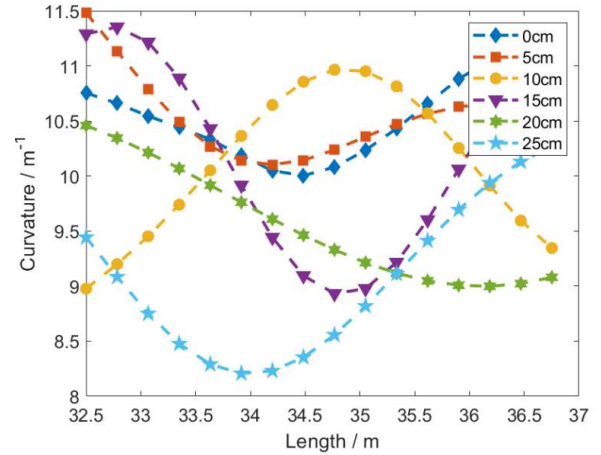


Fig. 4. Curvature values of the optical fiber ring at different water depths

TABLE I. MEAN CURVATURE AT DIFFERENT DEPTHS

Water depth	0cm	5cm	10cm	15cm	20cm	25cm
Curvature mean	10.53m ⁻¹	10.55m ⁻¹	10.11m ⁻¹	10.17m ⁻¹	9.54m ⁻¹	9.05m ⁻¹

In the experiment, the radius of the fiber ring is 9.5 cm, so the correspond true curvature value is 10.53 m⁻¹ ($\kappa = 1/R$), it can be seen from Fig. 4 that as the depth deepens, the fluctuation of the curvature value gradually increases, and all fluctuate along the length of the fiber around the curvature value of 10.53m⁻¹. In addition, according to the experimental results, it can be seen that when the water depth is deeper, the measured fiber curvature value is smaller. According to the experimental measurement data, a data fitting was performed on the measured curvature of the optical fiber at different water depth. The result is shown in Fig. 5. The horizontal axis represents the depth of the optical fiber underwater, the vertical axis represents the measured curvature value, and the fitted curve is the red curve in the graph.

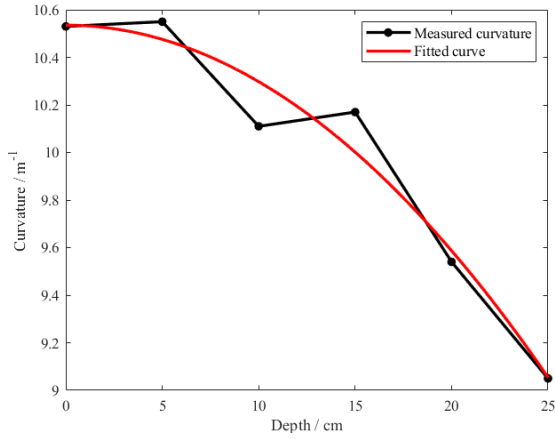


Fig. 5. Fitting of different depth curvature values of optical fiber

The fitting results show that the measured curvature value of the optical fiber has a quadratic function relationship with the depth. Based on the fitted curve, we can make corrections to the measured curvature values and the corrected results are shown in Fig. 6. It is also possible to calculate the correction error, the results of which are shown in Table II. From Table II, it can be seen that we can obtain the true curvature by correcting the measured curvature, and the correction effect becomes more significant as the position of the fibre in the water increases.

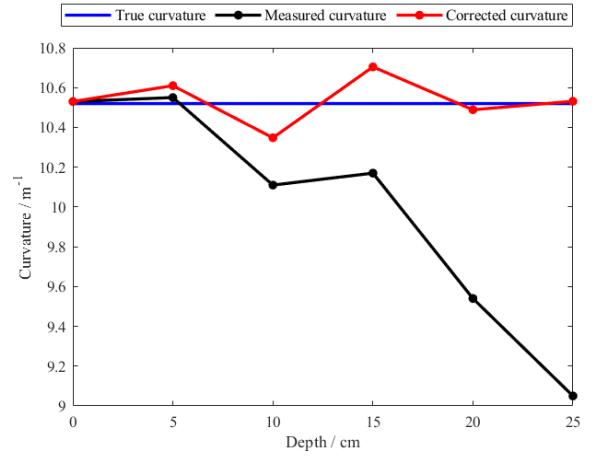


Fig. 6. The result after curvature correction

TABLE II. MAGNITUDE OF CURVATURE ERROR BEFORE AND AFTER CORRECTION

Water depth	0cm	5cm	10cm	15cm	20cm	25cm
Error before correction	0%	0.19%	3.99%	3.42%	9.40%	14.1%
Error after correction	0%	0.76%	1.71%	1.61%	0.38%	0.01%

V. CONCLUSION

Using multi-core fiber and OFDR system, data measurements in the underwater environment have been achieved. The correction of these data allowed the true curvature magnitude to be obtained, with a maximum error of 1.71% after correction, proving the feasibility of the experimental system in the underwater environment and providing an important reference for strain vector sensing in the deep-sea environment.

REFERENCES

- [1] M. Badar, T. Hino, and K. Iwashita, "Phase Noise Cancelled OFDR With cm-Level Spatial Resolution Using Phase Diversity," *IEEE Photon Technol Lett*, vol. 26, no. 9, pp. 858–861, May 2014.
- [2] G. Capilla-Gonzalez, D. A. May-Arrijo, D. Lopez-Cortes, and J. R. Guzman-Sepulveda, "Stress homogenization effect in multicore fiber optic bending sensors," *Appl Opt*, vol. 56, no. 8, p. 2273, Mar. 2017.
- [3] Z. Zhao, M. A. Soto, M. Tang, and L. Thévenaz, "Distributed shape sensing using Brillouin scattering in multi-core fibers," *Opt Express*, vol. 24, no. 22, p. 25211, Oct. 2016.
- [4] J. P. Moore, "Shape Sensing Using Multi-core Fiber," in *Optical Fiber Communication Conference*, Los Angeles, California, 2015, p. Th1C.2.
- [5] J. Cui, S. Zhao, C. Yang, and J. Tan, "Parallel Transport Frame for Fiber Shape Sensing," *IEEE Photon J*, vol. 10, no. 1, pp. 1–12, Feb. 2018.
- [6] M. D. Rogge and J. P. Moore, "Shape sensing using a multi-core optical fiber having an arbitrary initial shape in the presence of extrinsic forces" 2014.
- [7] C. Liang, Q. Bai, M. Yan, Y. Wang, H. Zhang, and B. Jin, "A Comprehensive Study of Optical Frequency Domain Reflectometry," *IEEE Access*, vol. 9, pp. 41647–41668, 2021.
- [8] J. Cui, S. Zhao, D. Yang, and Z. Ding, "Investigation of the interpolation method to improve the distributed strain measurement accuracy in optical frequency domain reflectometry systems," *Appl Opt*, vol. 57, no. 6, p. 1424, Feb. 2018.
- [9] F. Parent *et al.*, "Enhancement of accuracy in shape sensing of surgical needles using optical frequency domain reflectometry in optical fibers," *Biomed Opt Express*, vol. 8, no. 4, p. 2210, Apr. 2017.